Optics Letters

# Modulated coupled nanowires for ultrashort pulses

ALEXANDER S. SOLNTSEV* AND ANDREY A. SUKHORUKOV

*Nonlinear Physics Centre, Research School of Physics and Engineering, Australian National University, Canberra ACT 2601, Australia*
**Corresponding author: Alexander.Solntsev@anu.edu.au*

*Received 22 June 2015; revised 10 August 2015; accepted 11 August 2015; posted 11 August 2015 (Doc. ID 243462); published 26 August 2015*

**We predict analytically and confirm with numerical simulations that intermode dispersion in nanowire waveguide arrays can be tailored through periodic waveguide bending, facilitating flexible spatiotemporal reshaping without breakup of femtosecond pulses. This approach allows simultaneous and independent control of temporal dispersion and spatial diffraction that are often strongly connected in nanophotonic structures.** 

***OCIS codes:*** (080.1238) Array waveguide devices; (320.5540) Pulse shaping.

http://dx.doi.org/10.1364/OL.40.004078

Light control in dispersive coupled waveguides is an area of growing interest [1–6]. High-index-contrast nanowires based on semiconductors [7], glasses [8], and metals [9–11] offer unique advantages for the manipulation of optical pulses in compact photonic circuits, providing high field confinement and enabling precise dispersion engineering. In particular, optical chips based on silicon subwavelength waveguides allow for efficient frequency conversion [12,13], all-optical pulse control [14], and all-optical switching [15]. Furthermore, couplers [16] and arrays of coupled nanowire waveguides [17,18] open possibilities for efficient spatiotemporal shaping of optical pulses. In order to harness these opportunities, it is essential to develop approaches to simultaneously and independently control temporal and spatial dispersion, as these characteristics can be strongly connected in nanophotonic structures. This connectivity can lead to difficulties designing a waveguide array supporting propagation of ultrashort pulses, since pulses either disperse due to strong temporal dispersion or breakup due to strong spatial diffraction [18].

One possible approach to achieve required spatiotemporal dispersion is to carefully design waveguide array geometry and use complex photonic crystal structures [19]. However, that is a very complicated method. Another way to tailor dispersion is by introducing periodic waveguide bending [11,20,21]. This approach allows relatively simple fabrication and offers substantial design flexibility. Periodic waveguide bending was introduced as an effective tool for polychromatic diffraction management [20–22]; however, it has only been studied in the context of continuous light illumination and conventional microscale waveguides. In this work, we develop an approach to simultaneously control spatial and temporal dispersion and demonstrate through numerical simulations the application of this concept to the suppression of ultrashort pulse distortion and breakup in nanowaveguide arrays.

We analyze the propagation of ultrashort pulses in waveguide arrays associated with the excitation of only the fundamental modes of individual nanowires. Then, the spatiotemporal propagation dynamics can be modeled by coupled equations for the mode amplitudes [10]. Ultrashort pulses have a broad spectrum encompassing a large range of frequencies $\omega$. Therefore, temporal dispersion characterized by a propagation constant $\beta_s(\omega)$ has a significant influence on the pulse dynamics. In waveguide arrays pulses can also switch between different waveguides. One of the most important parameters characterizing waveguide arrays is a coupling coefficient $C_s(\omega)$, which determines the rate at which light couples between the neighboring waveguides and thus regulates the spatial dispersion. The coupling coefficient for straight lossless waveguides is real: $C_s(\omega) = \mathrm{Re}[C_s(\omega)]$.

In waveguide arrays with a relatively small waveguide curvature, when the mode profiles of individual nanowires are not perturbed, the coupled-mode approach is also applicable [11]. The main effect of bending appears to be due to the geometrical effect of tilting the mode phase fronts. This leads to the appearance of the effective phase shift in the coupling coefficients between the waveguides, which is directly proportional to the light frequency [21]. If all waveguides in an array have the same bending profile $x_0(z)$, where $x_0$ is a transverse coordinate of the waveguide center and $z$ is the propagation direction, then the complex electric field amplitude $E_n$ in $n$th waveguide of the array satisfies the following coupled-mode equations [21]:

$$\begin{aligned} &i\partial_z E_n(z,\omega) + \beta_s(\omega)E_n(z,\omega) \\ &= -C_s(\omega)\exp[in_0 d_w \dot{x}_0(z)\omega/c]E_{n-1}(z,\omega) \\ &\quad - C_s(\omega)\exp[-in_0 d_w \dot{x}_0(z)\omega/c]E_{n+1}(z,\omega). \end{aligned} \tag{1}$$

Here, $n_0$ is an effective refractive index, $\omega = 2\pi c/\lambda$ is the angular frequency, $\lambda$ is the light wavelength in vacuum, and $d_w$ is the distance between the coupled waveguides.

We extend this method to consider the dynamics of ultrashort pulses and study its applicability to nanophotonic

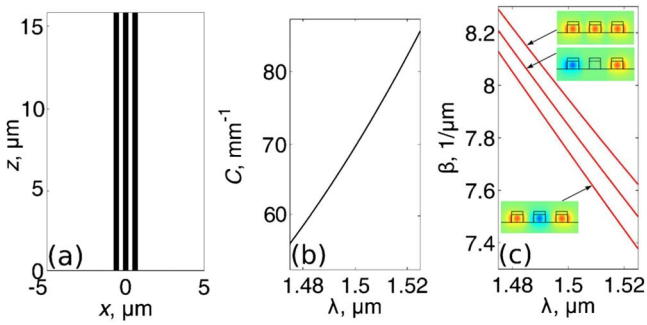


**Fig. 1.** (a) Scheme of three straight coupled nanowires. (b) Coupling coefficient versus wavelength between the neighboring waveguides. (c) Supermode propagation constants versus wavelength (solid lines), and the corresponding profiles of the dominant electric field x-components of the supermodes (cross sections of three coupled waveguides).

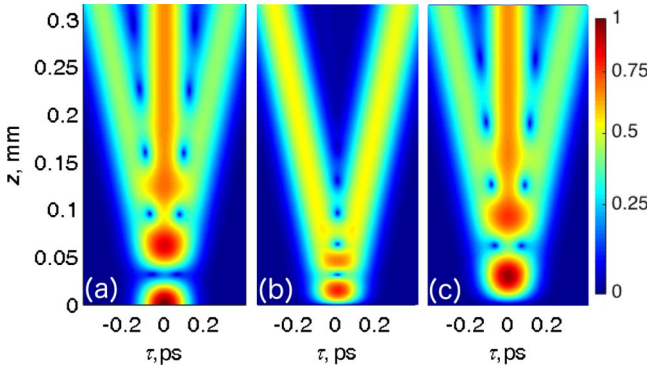


**Fig. 2.** Pulse intensity evolution along straight coupled nanowires: (a) left, (b) central, and (c) right nanowire. The temporal axis corresponds to a moving time frame with the group velocity at the central wavelength, $\tau = t - z\beta_1$.

structures. In low-index waveguide arrays both the propagation constant of individual waveguides and the coefficient characterizing coupling between the neighboring waveguides are mildly dispersive. In contrast, in nanowire high-index waveguides the dispersion can be much stronger, and also small changes in the waveguide cross section dramatically affect both temporal dispersion and spatial diffraction [18].

To investigate the pulse dynamics in the coupled nanowires, we combine the approaches previously developed for the description of nanowire arrays [18] and curved conventional waveguide arrays [20,22]. We derive the following system of equations by applying to Eq. (1) the Fourier transform $E_n(z,t) = \int d\omega E_n(z,\omega)\exp(-i\omega t)$, where $t$ is time, and perform a Taylor expansion of coupling and propagation coefficients:

$$i\partial_z E_n(z,t) + \hat{\beta}E_n(z,t) = -\hat{C}(z)E_{n-1}(z,t) - \hat{C}^*(z)E_{n+1}(z,t). \quad (2)$$

We note that this set of equations describes linear propagation of light, although it would be of interest to consider the extension of this method to include nonlinear effects in future works. Here, $\hat{\beta}$ determines the temporal dispersion in a waveguide, and $\hat{C}$ characterizes the coupling between the neighboring waveguides:

$$\hat{\beta} = \sum_{m=0}^{M} \frac{\beta_m}{m!}(i\partial_t)^m, \qquad \hat{C}(z) = \sum_{m=0}^{M} \frac{c_m(z)}{m!}(i\partial_t)^m, \quad (3)$$

where $M$ is a sufficiently large number to capture the dispersion features over the pulse bandwidth. The Taylor coefficients are

$$\beta_m = (\partial_\omega)^m \beta_s(\omega)|_{\omega=\omega_0},$$
$$c_m(z) = (\partial_\omega)^m [C_s(\omega)\exp(in_0 d_w \dot{x}_0(z)\omega/c)]_{\omega=\omega_0}, \quad (4)$$

where $\omega_0$ is the central pulse frequency. Note that the dispersion coefficients ($\beta_m$) do not depend on the coupling. On the other hand, the coupling coefficients ($c_m$) depend nontrivially on the propagation distance ($z$) through an interplay between the dispersion of coupling between the straight waveguides ($C_s$) and the bending profile [$x_0(z)$] induced dispersion.

It was shown [21] that for polychromatic light propagation in periodically curved waveguide arrays, after the full bending period the beam diffraction is the same as in a straight array with the effective coupling coefficient. We check that the same approach can be applied to the pulse propagation when $x_0(z) \equiv x_0(z + L_b)$ and $L_b$ is a modulation period, and the effective coupling is

$$C^{\text{eff}}(\omega) = C_s(\omega)L_b^{-1}\int_0^{L_b} \cos[n_0 d_w \dot{x}_0(z)\omega/c]\mathrm{d}z. \quad (5)$$

The corresponding Taylor expansion coefficients are

$$c_m^{\text{eff}} = (\partial_\omega)^m C^{\text{eff}}(\omega)|_{\omega=\omega_0}. \quad (6)$$

We see that diffraction of beams is defined by an interplay of the additional bending-induced dispersion introduced through the frequency dependence of the integral in Eq. (5), and the intrinsic frequency dependence of the coupling coefficient in a straight waveguide array $C_s(\omega)$.

We investigate the influence of the periodic waveguide bending on the pulse reshaping and consider a representative example of a cosine profile with the amplitude $A$ and period $L_b$:

$$x_0(z) = A\cos(2\pi z/L_b). \quad (7)$$

The cosine profile enables flexible control of linear dispersion while avoiding sharp bends. Below we show that a special combination of the modulation parameters allows us to suppress the dispersion of the effective coupling coefficient and accordingly avoid the pulse distortion.

To demonstrate our approach, we consider coupled Si nanowire waveguides and use the COMSOL RF module for vectorial calculations of linear electromagnetic modes and their dispersion, while fully taking into account transverse and longitudinal field components. These calculations allow us to find the propagation and coupling constants introduced in Eq. (6). We focus on gradual bending that preserves the overall vectorial structure of the modes and does not introduce additional losses. The wires are 220 nm high and 330 nm wide, placed on a silica slab. There is a 100 nm high etching mask with a refractive index of 1.35 on top of wires. Otherwise, the wires are surrounded by air. We choose these parameters to obtain nearly zero group velocity dispersion $\beta_2 \approx 0$ in the proximity of $\lambda_0 = 1.5$ μm wavelength for a single nanowire, as this would minimize the pulse distortion. However, we emphasize that

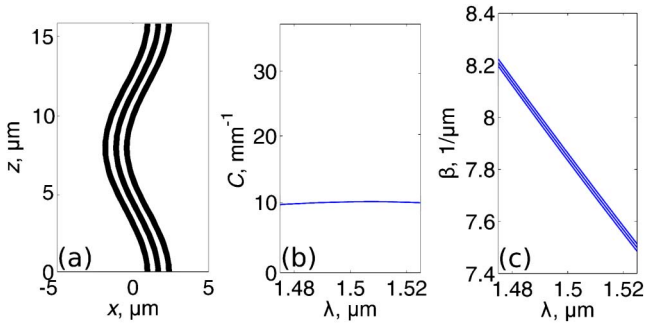


**Fig. 3.** (a) The scheme of three periodically bent coupled nanowires with the bending period $L_b = L_C = 15.75$ μm. (b) Effective coupling coefficient over one bending period between the neighboring nanowires versus wavelength. (c) Average supermode propagation constants over one bending period versus wavelength.

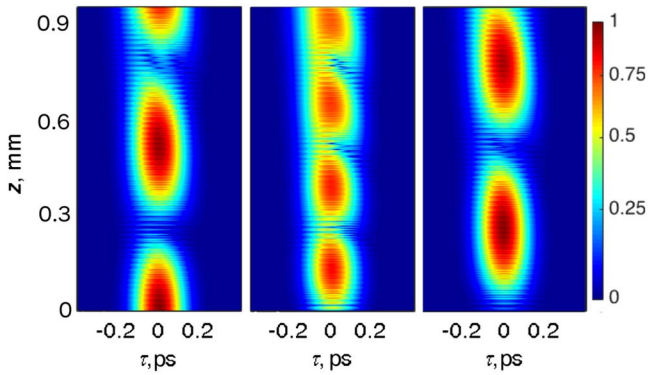


**Fig. 4.** Pulse intensity evolution along periodically curved coupled nanowires: (a) left edge nanowire, (b) central nanowire, and (c) right edge nanowire. The temporal axis corresponds to a moving time frame with the group velocity at the central wavelength, $\tau = t - z\beta_1$. The length of the modulated waveguide array has been increased by a factor of three compared to the straight waveguide array to show that the dispersion is mostly compensated even at longer distances.

even in this regime, a pulse can exhibit distortion in an array of nanowires due to the dispersion of coupling [18].

To determine the coupling strength between the neighboring waveguides, we follow the approach of Ref. [18] and analyze a two-waveguide coupler with wire-to-wire separation of 330 nm. We calculate the propagation constants for symmetric and antisymmetric supermodes of the coupler, $\beta^{\text{sym}}(\omega)$ and $\beta^{\text{asym}}(\omega)$, respectively. The propagation constant for a single waveguide can be well approximated by the average of the symmetric and antisymmetric supermode propagation constants $\beta_s(\omega) \approx [\beta^{\text{sym}}(\omega) + \beta^{\text{asym}}(\omega)]/2$, while the difference defines the coupling coefficient $C_s(\omega) = [\beta^{\text{sym}}(\omega) - \beta^{\text{asym}}(\omega)]/2$. The coefficients of the Taylor expansion of the propagation constant are found as $\beta_0 = 7.85\ \mu\text{m}^{-1}$, $\beta_1 = 17\ \text{fs}\,\mu\text{m}^{-1}$, and $\beta_2 = 1.4\ \text{fs}^2\,\mu\text{m}^{-1}$. Accordingly, we find that the group velocity dispersion is indeed largely suppressed for pulses with duration down to 100 fs propagating in sub-mm long structures. We also check that higher-order dispersion does not substantially affect such pulses at these distances.

To show that our approach works not only with two-waveguide couplers, we choose a three-waveguide structure for the following illustrations with all parameters as noted before; see Fig. 1(a). We note that this method works well with an arbitrary number of waveguides. In agreement with predictions of Ref. [18], we notice that the variations of the coupling coefficient for such waveguide arrays are significant across a relatively narrow spectrum [see Fig. 1(b)], which could lead to temporal reshaping of short pulses during propagation. The Taylor expansion of the coupling coefficient for straight waveguides is $c_0 = 69.7\ \text{mm}^{-1}$, $c_1 = -0.71\ \text{fs}\,\mu\text{m}^{-1}$, and $c_2 = 3.6\ \text{fs}^2\,\mu\text{m}^{-1}$, which reveals strong linear dispersion and small quadratic dispersion in the wavelength range between 1.46 and 1.54 μm. The coupled waveguides support three supermodes, and we present the calculated dependence of their propagation constants on the wavelength in Fig. 1(c). The insets show the characteristic spatial profiles of the supermodes. The dispersion dependencies have different slopes corresponding to different supermode velocities. We show below that this leads to pulse splitting, which can be suppressed via periodic waveguide bending.

First, we analyze the pulse dynamics in straight waveguides with length $L = 20L_C = 315$ μm, where $L_C = 15.75$ μm is the length required for full coupling from one waveguide to another at the wavelength $\lambda_0$. As an input, we consider a single 100 fs long nonchirped Gaussian pulse with the central wavelength $\lambda_0$ coupled to the left nanowire of the straight waveguide array. Figures 2(a)–2(c) demonstrate that initially the pulse couples from the left (a), to the central (b), and then to right (c) nanowire without significant distortions. Then the pulse starts to split into three separate pulses in the edge waveguides [(a) and (c)] and into two pulses in the central waveguide (b), in agreement with the previous study [18]. These pulses propagate with different group velocities, which correspond to three different supermode velocities supported in the structure [see Fig. 1(c)]. Such behavior demonstrates that although the single nanowire dispersion can be engineered, spatial diffraction in arrays of nanowires is still strongly affected by the coupling dispersion. Moreover, the supermode dispersion and the coupling dispersion in nanowire waveguide arrays are interconnected. Therefore, an approach allowing for the independent control of these characteristics would offer essential benefits for various applications.

Next, we investigate the influence of the periodic waveguide bending on the pulse reshaping. We choose a bending profile according to Eq. (7). We vary the bending amplitude $A$ and search for the minima of the coupling dispersion $\partial C_{\text{eff}}/\partial\omega$ in the vicinity of $\lambda_0$. We choose the bending period $L_b = L_C = 15.75$ μm, as it allows us to consider nanowires with smaller curvature for the purposes of easier potential fabrication and reduction of propagation losses. As we show below, one can choose a bending profile that simultaneously allows for a strong coupling dispersion control and does not introduce bending propagation losses.

We calculate the effective coupling coefficient $C_{\text{eff}}$ using Eq. (5). We choose the value of $A = A_{\text{min}}$ corresponding to the first minimum of $\partial C_{\text{eff}}/\partial\omega$ and accordingly the smallest suitable bending curvature. The optimal bending amplitude is found to be equal to $A_{\text{min}} = 1.3$ μm. The bending losses for the corresponding curvature value should be practically absent according to the previous studies of bent nanowire waveguides [23]. The resulting effective coupling coefficient $C_{\text{eff}}$

shown in Fig. 3(b) becomes almost constant over a broad spectral region in comparison to that for the straight waveguides [c.f. Fig. 1(b)]. The Taylor expansion of the effective coupling coefficient is $c_0^{\text{eff}} = 9.96\ \text{mm}^{-1}$, $c_1^{\text{eff}} = -0.0076\ \text{fs}\,\mu\text{m}^{-1}$, and $c_2^{\text{eff}} = -14.2\ \text{fs}^2\,\mu\text{m}^{-1}$. Although the quadratic coupling dispersion is slightly increased in comparison to the straight waveguide array, the linear coupling dispersion, which is the main temporal reshaping driver for 100 fs long pulses in such structures, is suppressed by two orders of magnitude compared to the straight waveguides. In Fig. 3(c), we plot the supermode propagation constants for the curved waveguide arrays with three coupled nanowires calculated with the use of the effective coupling coefficient. The propagation constants for the three supermodes now have similar slopes, which suggests that short-pulse breakup due to coupling would be suppressed.

We now calculate the intensity evolution of a 100 fs transform-limited pulse coupled to the left nanowire of the periodically curved waveguide array using the Eqs. (2)–(4). We show in Figs. 4(a)–4(c) that as a result of vanishing coupling dispersion the temporal pulse breakup is suppressed, and a pulse can now be switched as a whole between the waveguides. Thus, the temporal and the spatial dispersion in nanowire waveguide arrays can be controlled independently via single waveguide dispersion engineering and periodic waveguide bending.

These results demonstrate that spatiotemporal dispersion engineering in high-index-contrast nanowire waveguide arrays can be efficiently realized through the introduction of periodic waveguide bending, which can enable flexible spatiotemporal manipulation of femtosecond pulses. We anticipate that these results will open novel approaches to on-chip all-optical light control [17]. This approach can also be useful for enhanced parametric frequency conversion [8] and broadband photon-pair generation and quantum walks [24].

**Funding.** Australian National Computational Infrastructure Facility; Australian Research Council (ARC) (DP130100086, FT100100160).

## REFERENCES

1. K. S. Chiang, Opt. Lett. **20**, 997 (1995).
2. K. S. Chiang, IEEE J. Quantum Electron. **33**, 950 (1997).
3. P. M. Ramos and C. R. Paiva, IEEE J. Quantum Electron. **35**, 983 (1999).
4. V. Rastogi, K. S. Chiang, and N. N. Akhmediev, Phys. Lett. A **301**, 27 (2002).
5. M. Liu and K. S. Chiang, IEEE J. Quantum Electron. **47**, 1499 (2011).
6. Y. V. Kartashov, B. A. Malomed, V. V. Konotop, V. E. Lobanov, and L. Torner, Opt. Lett. **40**, 1045 (2015).
7. A. C. Turner, C. Manolatou, B. S. Schmidt, M. Lipson, M. A. Foster, J. E. Sharping, and A. L. Gaeta, Opt. Express **14**, 4357 (2006).
8. M. A. Foster, A. C. Turner, M. Lipson, and A. L. Gaeta, Opt. Express **16**, 1300 (2008).
9. Y. M. Liu, G. Bartal, D. A. Genov, and X. Zhang, Phys. Rev. Lett. **99**, 153901 (2007).
10. F. Ye, D. Mihalache, B. Hu, and N. C. Panoiu, Phys. Rev. Lett. **104**, 106802 (2010).
11. G. Della Valle and S. Longhi, Opt. Lett. **35**, 673 (2010).
12. M. A. Foster, A. C. Turner, J. E. Sharping, B. S. Schmidt, M. Lipson, and A. L. Gaeta, Nature **441**, 960 (2006).
13. A. S. Solntsev and A. A. Sukhorukov, Opt. Lett. **37**, 446 (2012).
14. V. R. Almeida, C. A. Barrios, R. R. Panepucci, and M. Lipson, Nature **431**, 1081 (2004).
15. Y. Vlasov, W. M. J. Green, and F. Xia, Nat. Photonics **2**, 242 (2008).
16. C. E. de Nobriga, G. D. Hobbs, W. J. Wadsworth, J. C. Knight, D. V. Skryabin, A. Samarelli, M. Sorel, and R. M. De La Rue, Opt. Lett. **35**, 3925 (2010).
17. O. Peleg, M. Segev, G. Bartal, D. N. Christodoulides, and N. Moiseyev, Phys. Rev. Lett. **102**, 163902 (2009).
18. C. J. Benton and D. V. Skryabin, Opt. Express **17**, 5879 (2009).
19. J. Laegsgaard, O. Bang, and A. Bjarklev, Opt. Lett. **29**, 2473 (2004).
20. I. L. Garanovich and A. A. Sukhorukov, Opt. Lett. **32**, 475 (2007).
21. I. L. Garanovich, S. Longhi, A. A. Sukhorukov, and Y. S. Kivshar, Phys. Rep. **518**, 1 (2012).
22. A. Szameit, I. L. Garanovich, M. Heinrich, A. A. Sukhorukov, F. Dreisow, T. Pertsch, S. Nolte, A. Tuennermann, and Y. S. Kivshar, Nat. Phys. **5**, 271 (2009).
23. D. X. Dai and Z. Sheng, J. Opt. Soc. Am. B **24**, 2853 (2007).
24. A. S. Solntsev, A. A. Sukhorukov, D. N. Neshev, and Y. S. Kivshar, Opt. Express **20**, 27441 (2012).